REPORT DOCUMENTATION PAGE

Form Approved OMB NO. 0704-0188

1. REPORT DATE (DD-MM-YYYY)	2. REPORT TYPE	3. DATES COVERED (From - To)
18-03-2017	Final Report	28-Sep-2015 - 27-Jun-2016

4. TITLE AND SUBTITLE
Final Report: Mitigating the loss in plasmonics and metamaterials

5a. CONTRACT NUMBER
W911NF-15-1-0629

5b. GRANT NUMBER

5c. PROGRAM ELEMENT NUMBER
611102

6. AUTHORS
Jacob B Khurgin

5d. PROJECT NUMBER

5e. TASK NUMBER

5f. WORK UNIT NUMBER

7. PERFORMING ORGANIZATION NAMES AND ADDRESSES
Johns Hopkins University
3400 N. Charles St
Malone 146
Baltimore, MD 21218 -2608

8. PERFORMING ORGANIZATION REPORT NUMBER

9. SPONSORING/MONITORING AGENCY NAME(S) AND ADDRESS (ES)
U.S. Army Research Office
P.O. Box 12211
Research Triangle Park, NC 27709-2211

10. SPONSOR/MONITOR'S ACRONYM(S)
ARO

11. SPONSOR/MONITOR'S REPORT NUMBER(S)
68173-EL-II.8

12. DISTRIBUTION AVAILIBILITY STATEMENT
Approved for Public Release; Distribution Unlimited

13. SUPPLEMENTARY NOTES
The views, opinions and/or findings contained in this report are those of the author(s) and should not contrued as an official Department of the Army position, policy or decision, unless so designated by other documentation.

14. ABSTRACT

Abstract
Current materials of choice for plasmonics and metamaterials (P&M) are mostly metals, but also highly doped semiconductors, oxides and nitrides. The common feature of all these materials is high loss determined by absorption in which photon (or surface plasmon) gets absorbed and its energy is transferred to electron-hole pair. While there are many extrinsic factors that may increase or decrease the absorption strength (defects, roughness, strength of electron-phonon coupling etc.), fundamentally the absorption in the materials with large density of free

15. SUBJECT TERMS
Plasmonics, Loss, Polaritons, Metals, Semiconductors

16. SECURITY CLASSIFICATION OF:			17. LIMITATION OF ABSTRACT	15. NUMBER OF PAGES	19a. NAME OF RESPONSIBLE PERSON
a. REPORT	b. ABSTRACT	c. THIS PAGE			Jacob Khurgin
UU	UU	UU	UU		19b. TELEPHONE NUMBER 410-516-7518

Report Title

Final Report: Mitigating the loss in plasmonics and metamaterials

ABSTRACT

Abstract
Current materials of choice for plasmonics and metamaterials (P&M) are mostly metals, but also highly doped semiconductors, oxides and nitrides. The common feature of all these materials is high loss determined by absorption in which photon (or surface plasmon) gets absorbed and its energy is transferred to electron-hole pair. While there are many extrinsic factors that may increase or decrease the absorption strength (defects, roughness, strength of electron-phonon coupling etc.), fundamentally the absorption in the materials with large density of free carriers is high because of the large density of final states for the absorption. In the course of 9 month of work we have investigated various means of loss mitigation using alternative materials , such as heavily doped semiconductors, oxides and phononic materials. Despite lower material losses the polaritonic modes in these materials turned outto be just as lossy if not lossier than in the metals which we have attributed to the lower plasma frequency ion the alternative materials. The one and only way to have material with negative dielectric constant ? and low absorption is to synthesize a material in which the absorption would be forbidden by the energy conservation. We have identified two dimensional layered materials as potential candidates and approached a research group at DTU (Denmark) whose density functional calculations confirmed our prediction.

Enter List of papers submitted or published that acknowledge ARO support from the start of the project to the date of this printing. List the papers, including journal references, in the following categories:

(a) Papers published in peer-reviewed journals (N/A for none)

Received		Paper
02/22/2017	1	Jacob B. Khurgin. Replacing noble metals with alternative materials in plasmonics and metamaterials: how good an idea?, Philosophical Transactions of the Royal Society A: Mathematical, Physical and Engineering Sciences, ( ): 20160068. doi:
02/22/2017	2	Sergey I. Bozhevolnyi, Jacob B. Khurgin. Fundamental limitations in spontaneous emission rate of single-photon sources, Optica, ( ): 1418. doi:
02/22/2017	3	Tengfei Li, Jacob B. Khurgin. Hyperbolic metamaterials: beyond the effective medium theory, Optica, ( ): 1388. doi:
TOTAL:	**3**	

Number of Papers published in peer-reviewed journals:

(b) Papers published in non-peer-reviewed journals (N/A for none)

Received	Paper
TOTAL:	

Number of Papers published in non peer-reviewed journals:

(c) Presentations

Replacing Metals with Alternative Plasmonic Substances in Plasmonics and Metamaterials: is it a good idea? Jacob B Khurgin
10th International Congress on Advanced Electromagnetic Materials in Microwaves and Optics – Metamaterials 2016
Crete, Greece, 17-22 September 2016

Number of Presentations: 3.00

Non Peer-Reviewed Conference Proceeding publications (other than abstracts):

Received	Paper
03/08/2017	4 Tengfei Li, Jacob B Khurgin. What are the merits of hyperbolic metamaterials?, CLEO: QELS_Fundamental Science. 05-JUN-16, San Jose, California. : ,
03/08/2017	5 Jacob B Khurgin, Greg Sun. Limits of plasmonic enhancement: what if the metal becomes “lossless”?, CLEO: QELS_Fundamental Science. 05-JUN-16, San Jose, California. : ,
TOTAL:	**2**

Number of Non Peer-Reviewed Conference Proceeding publications (other than abstracts):

Peer-Reviewed Conference Proceeding publications (other than abstracts):

Received	Paper
TOTAL:	

Number of Peer-Reviewed Conference Proceeding publications (other than abstracts):

(d) Manuscripts

Received	Paper
TOTAL:	

Number of Manuscripts:

Books

Received Book

TOTAL:

Received Book Chapter

03/08/2017 7.00 Jacob B Khurgin. Landau Damping—The Ultimate Limit of Field Confinement and Enhancement in Plasmonic Structures, Switzerland: Springer, (2017)

TOTAL: **1**

Patents Submitted

Patents Awarded

Awards

Graduate Students

NAME	PERCENT_SUPPORTED

FTE Equivalent:
Total Number:

Names of Post Doctorates

NAME	PERCENT_SUPPORTED

FTE Equivalent:
Total Number:

Names of Faculty Supported

NAME	PERCENT_SUPPORTED

FTE Equivalent:
Total Number:

Names of Under Graduate students supported

NAME	PERCENT_SUPPORTED

FTE Equivalent:
Total Number:

Student Metrics

This section only applies to graduating undergraduates supported by this agreement in this reporting period

The number of undergraduates funded by this agreement who graduated during this period:	0.00
The number of undergraduates funded by this agreement who graduated during this period with a degree in science, mathematics, engineering, or technology fields:.....	0.00
The number of undergraduates funded by your agreement who graduated during this period and will continue to pursue a graduate or Ph.D. degree in science, mathematics, engineering, or technology fields:.....	0.00
Number of graduating undergraduates who achieved a 3.5 GPA to 4.0 (4.0 max scale):.....	0.00
Number of graduating undergraduates funded by a DoD funded Center of Excellence grant for Education, Research and Engineering:.....	0.00
The number of undergraduates funded by your agreement who graduated during this period and intend to work for the Department of Defense	0.00
The number of undergraduates funded by your agreement who graduated during this period and will receive scholarships or fellowships for further studies in science, mathematics, engineering or technology fields:	0.00

Names of Personnel receiving masters degrees

NAME

Total Number:

Names of personnel receiving PHDs

NAME

Total Number:

Names of other research staff

NAME	PERCENT_SUPPORTED

FTE Equivalent:
Total Number:

Sub Contractors (DD882)

Inventions (DD882)

Scientific Progress

See Attachement

Technology Transfer

Scientific Progress and Accomplishments

Table of Contents:

Statement of the problems studied

In the course of the short project with limited time frame we have performed research along the
following directions.

- Possibility of using highly doped semiconductors, nitrides and oxides as a substitute for the noble metals, especially in the near infrared range of materials.
- Using phonon polaritons for performing the same tasks as plasmonics but with lower loss
- Study of the effect of landau damping on maximum field enhancement attainable with the plasmonic dimers and nanoantennas
- Investigation of the possibility of creating a chemically stable lossless metal with Van-der-Waals materials.

Summary of the most important results

Based on the results of our research we have made the following conclusions:

(a) The noble metals, imperfect as they are, still hold advantage over all the alternative material, largely due to the fact that have larger density of free carriers (plasma frequency). In this sense it is the overall conductance of the structure rather than the mobility that determines the loss.

(b) Phonon polaritons do hold advantage over the doped semiconductors and metals when it comes to material loss but the enhancement of the electric field is not as strong as expected

(c) In the end, even if the scattering loss due to phonons, impurities and imperfections is eliminated entirely, Landau damping negates all the progress for really small structures

(d) We have identified a group in Denmark that has shown that it is possible to achieve a zero loss in a limited spectral range using a new class of two dimensional materials

Detailed report

1. Novel plasmonic materials: do they make sense?

Metals, which dominate the fields of plasmonics and metamaterials suffer from large ohmic losses. New plasmonic materials, such as doped oxides and nitrides, have smaller material loss, and using them in place of metals carries a promise of reduced-loss plasmonic and metamaterial structures, with sharper resonances and higher field concentration. This promise is now put to a rigorous analytical test in this work and it is revealed that having low material loss is not sufficient to have a reduced modal loss in plasmonic structures, unless the plasma frequency is significantly higher than the operational frequency. Using examples of nanoparticle plasmons and gap plasmons one comes to the conclusion that even in the mid-infrared spectrum metals continue to hold advantage over the alternative media. The new materials may still find application niche where the high absorption loss is beneficial, e.g. in medicine and thermal photovoltaics.

1.a Kinetic and Magnetic Inductances

Plasmonics and closely related to it filed of metamaterials have been among the most active and exciting areas of optical sciences over the last decade [1]. The innate ability of plasmonic structures to squeeze optical energy into subwavelength volumes and

thus achieve high degree of energy concentration allows one to enhance various linear, and especially nonlinear optical processes. This ability makes surface plasmon polariton (SPP) modes attractive candidates for use in applications like bio- and environmental sensing, photovoltaics, nonlinear optics, light sources, and all other areas where the extreme localization of electromagnetic fields can improve efficiency, speed, or both. Propagating SPP's in sub-wavelength structures have been long promoted as the candidates for the future on-chip optical interconnects. Metamaterials and metasurfaces relying on plasmonic resonances have been envisioned as the building elements of novel optical systems with widely extended functionality, such as super lenses and optical cloaks.

The lofty promise of plasmonics and metamaterials has not been yet fulfilled and the main reason for it lies in extremely high ohmic loss in all metals, even the noble ones that are currently the mainstay of plasmonics and metamaterials. The salient feature of all the metals is the negative real part of the dielectric constant,

$$\varepsilon_r = 1 - \omega_p^2 / \left(\omega^2 + i\omega\gamma \right) \tag{1}$$

where ω_p is the plasma frequency and γ is the momentum scattering rate, responsible for the loss. For frequencies $\omega < \omega_p$ the subwavelength confinement is achievable in the SPP modes of various metal-dielectric structures. Sub-λ confinement is enabled by the fact that In these modes the energy oscillates between the electrical energy and the kinetic energy of free electrons, with only a small fraction of energy contained in the magnetic form. However, as explained in [2] the energy contained in the form of kinetic motion is dissipated with the rate γ, hence the total energy of the SPP mode also decays at the rate commensurate with $\gamma \approx 10^{14} s^{-1}$. Thus the higher confinement always leads to higher loss, at least in the visible spectrum.

Therefore in the last few years the effort to develop *alternative plasmonic materials*, such as strongly doped semiconductors (InGaAs, ITO, AlZnO,) as well as nitrides (TiN, ZrN) and others [3,4]. In general, all of these materials have smaller ω_p then noble metals which precludes their application at short wavelengths. But at the same time some of them especially III-V materials have scattering rates that are lower by as much as an order of magnitude than those of the metals. This relation is natural, since plasma frequency increases as the Fermi surface expands in the k-space, but as the area of

the Fermi surface increases, so does the density of states into which the electrons can scatter by various mechanisms, *hence γ increases in step with* ω_p.

The low loss of the alternative materials makes them attractive for applications in the near and mid-infrared region [3,4], but at this point experimental data do not support this projection. While part of the problem is in fabrication difficulties, recent numerical analysis [5] has shown that all said and done, when it comes to the loss, Ag is still superior to all new plasmonic materials, including graphene. In this work we look into the same issue analytically and determine that the main reason for so-far-disappointing performance of "new" materials is the low value of plasma frequency in them.

1.b Kinetic and Magnetic inductances

To understand the loss one shall consider the energy balance in the plasmonic mode [4]. Half of the time, all the energy is stored in the form of the electrical energy whose density is $U_e = \frac{1}{2}\varepsilon_0\varepsilon_r E^2 \cos^2 \omega t$. The other half time the energy is split between the magnetic energy with density $U_m = \frac{1}{2}\mu_0 H^2 \sin^2 \omega t$ and kinetic energy of the collective motion free electrons $U_k = \frac{1}{2} Nmv^2 \sin^2 \omega t$. Obviously $\int U_e dV = \int (U_m + U_k) dV$ and as the mode size decreases below λ the magnetic field gets progressively smaller (in accordance to the so-called quasi-static regime) and the relative fraction of the kinetic energy increases. Since kinetic energy is damped to the at a rate 2γ, it is not difficult to see that the effective rate of energy loss in the mode is

$$\gamma_{eff} = \gamma \frac{\int U_k dV}{\int (U_m + U_k) dV} \tag{2}$$

The total amount of magnetic energy in the mode is related to the conductivity current as $\int U_m dV = \frac{1}{2} L_m I^2$, where L_m is magnetic inductance. Similarly, one can introduce the *kinetic inductance* as $\int U_k dV = \frac{1}{2} L_k I^2$, and obtain from (2)the main expression for the effective loss $\gamma_{eff} = \gamma(1 + L_m / L_k)^{-1}$

1.c Loss scaling in the cylindrical plasmonic mode

Consider now the SPP mode around elliptical nanoparticle which we can approximate as a cylinder of length *l* and diameter *a* (Fig1.a). The length l can be adjusted to achieve

an SPP resonance at a given wavelength λ no matter what is ω_p. The electric field, and hence current, penetrates the metal by the skin depth, roughly $\lambda_p/2\pi$ where λ_p is the plasma wavelength. Therefore, the effective in which the current is contained is

$$S_{eff} = \frac{\pi a^2}{4}\left[1+\left(\frac{\pi a}{2\lambda_p}\right)^2\right]^{-1/2} \tag{3}$$

The total kinetic energy is $\int U_k dV = \frac{1}{2} N m v^2 S_{eff} l = \frac{1}{2} m I^2 l / N e^2 S_{eff}$,and, using definition of plasma frequency we obtain

$$L_k = l/\varepsilon_0 \omega_p^2 S_{eff} = \mu_0 l \lambda_p^2 / 4\pi^2 S_{eff} \tag{4}$$

As one can see, kinetic inductance depends only on the ratio between the plasma wavelength and the mode dimension *a*. The magnetic inductance exhibits only very weak dependence on the size *a*,

$$L_m = \frac{\mu_0}{2\pi} l\left[\log\left(\frac{4l}{a}\right)-1\right] \tag{5}$$

Thus we obtain a very simple relation between the two inductances and then the value of effective loss rate

$$\gamma_{eff} \approx \gamma / \left(1+2x^2/\sqrt{x^2+1}\right) \tag{6}$$

where $x = \pi a / 2\lambda_p$. The effective loss, and therefore broadening and maximum field enhancement do not depend on the wavelength of light, but only on the plasma wavelength. It is conceivable therefore that metal with larger γ and smaller λ_p would have smaller loss than a doped semiconductor. As one can see from the Fig. 1b, where the effective loss is plotted for the case of subwavelength structure a=λ/10, the effective loss for the metal (Au) is always higher than that for ITO even though ITO has lower material loss. In the end at long wavelength the effective loss is simply $\gamma_{eff} \approx \gamma\lambda_p / \pi a$, hence the *proper figure of merit for the material is* ω_p / γ .

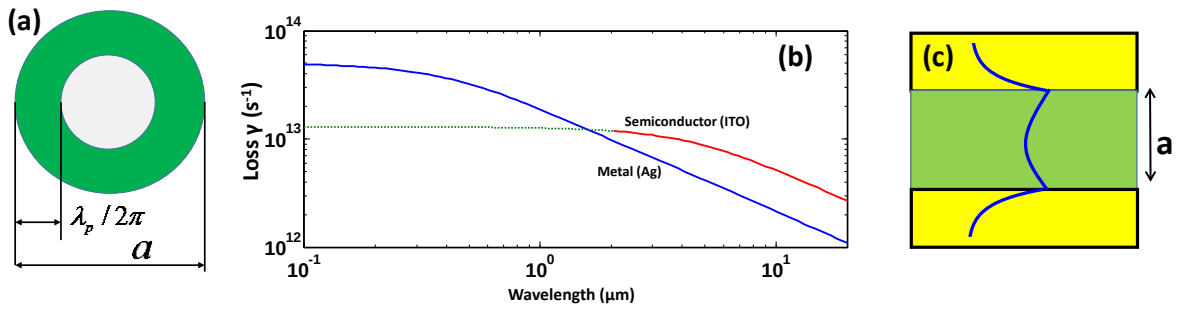

Fig. 1. (a) Cylindrical nanoparticle (b) Effective loss of the nanoparticle SPP for metal (Ag) and "new Plasmonic material" (ITO) (c) Gap plasmon

1.d Loss scaling in the gap plasmonic mode

One can extend this comparison to the case of the gap plasmon with the dielectric of thickness *a* confined between the metal or other plasmonic material as shown in Fig.1 c. After some algebra one can find the dispersive relation for the plasmon under assumption that effective propagation constant β is not significantly different from the wavevector in dielectric k_d which is a typical practical arrangement.

$$\beta = k_d + \frac{\omega}{\omega_p a}(1 + j\gamma / 2\omega) \tag{7}$$

The propagation length then cab be found as

$$L_{prop}^{-1} = \frac{\gamma n_d}{\omega_p a} = \frac{\lambda_p \gamma n_d}{2\pi c a} \tag{8}$$

where n_d is the index of dielectric. Once again, the loss depends only on the ratio $\pi a / \lambda_p$ and the figure of merit is ω_p / γ. *It is easy to see that the noble metals have higher FOM than most if not all "new" plasmonic material all the way to far IR range*, just as numerical simulations in Ref [5] have shown.

1.e Conclusions

To conclude this part, we have compared performance of the alternative plasmonic materials in the IR region with that of the metal and that the proper figure of merit, defining loss, broadening and field enhancement should be the ratio of plasma frequency ω_p and material loss γ. In laymen terms it indicates that it is always preferable to have

many electrons moving relatively slow rather than a few fast electrons. The figure of merit of all the new materials is worse than that of Ag and even Au. Therefore one cannot expect better performance from the new materials, which does not preclude their use where the loss, of propagation length, or degree of field enhancement is not the most important factor and new material may find their application niche simply due to the price and fabrication considerations.

2. Can one use phonon polaritons in place of metals in mid and far IR?

2.a Introduction

The common feature of various plasmonic schemes is their ability of confining optical fields of surface plasmon polaritons (SPPs) into sub-wavelength volumes and thus achieving large enhancement of linear and nonlinear optical properties. This ability, however, is severely limited by the large ohmic loss inherent to even the best of metals. In the mid and far infrared region of spectrum there exists an alternative to metals – polar dielectrics and semiconductors in which dielectric permittivity (real part) turns negative in the Reststrahlen region. This feature engenders the so-called surface phonon polaritons (SPhPs) capable of confining the field akin their plasmonic analogues, the SPPs. Since the damping rate of polar phonons is substantially less than that of free electrons in metal or semiconductor, it is not unreasonable to expect that "Phononic" devices may outperform their plasmonic counterparts. However, a more rigorous detailed analysis of comparative merits of Phononics and plasmonics reveals a more nuanced answer, namely that while Phononic schemes do exhibit narrower resonances and can achieve very high degree of **energy** concentration, most of the energy is contained in the form of lattice vibrations so that the enhancement of **electric field** and hence Purcell factor are rather small compared to what can be achieved with metal nanoantennas. Still, the sheer narrowness of SPhP resonances may make Phononics useful in the applications where frequency selectivity is important.

The discipline of optics for most of its existence has relied on a very limited sense of optical materials, mostly dielectrics with narrow range of refractive indices, from about 1.38 for MgF_2 to about 2.4 for TiO_2 in the visible and 4 for Ge in the near and mid-infrared. Consequently, the minimum size of optical components has been historically limited by the diffraction limit to about λ/n, i.e. few hundred nanometers making the

density of optical integration much lower than the density of electronic integration. In the course of the last decade-and-half the situation slowly started to change as the palette of optical materials has been expanded to include the material with negative permittivity (i.e. imaginary refractive index), mostly metals but also doped semiconductors, and a new discipline, plasmonics has emerged, free of the constraints imposed by the diffraction limit. At about the same time the optics community has realized that by combining sub-wavelength parts made from materials with different signs of permittivity, entirely new artificial media with properties that are unattainable in natural materials can be synthesizes. These media have been named "metamaterials" and a number of exciting potential applications for them, ranging from superlensing to optical cloaking have emerged. But after a few giddy years of unlimited promise the research in metamaterials and plasmonics has hit the wall as the community has started to recognized the obvious fact that ohmic loss in the metal prevents plasmonic and metamaterial devices from properly performing their functions. Once this unfortunate yet unavoidable fact has settled in, the research has slowly migrated towards the areas where the loss may not be the deciding factor (plasmonic sensors) or where it can in fact be useful (photo-catalysis, thermal photovoltaics an others). It was also suggested that loss can be mitigated by optical amplification, but it was shown the loss is simply too large for that and introduction of gain medium only increases noise. Hence the main hope for plasmonics and metamaterials use in such applications as integrated optics lies in discovering or developing new low loss material systems.

While in the visible and near IR range it is very difficult to find an alternative to the noble metal (and not for the lack of trying!) the situation in the mid-IR –to-THZ range appears to be far more promising [6]. The scattering rates in the highly doped semiconductors are on the order of $10^{13}s^{-1}$, i.e. about an order of magnitude less than in the metals, however the plasma frequency is also significantly less, i.e. skin depth in semiconductors is much larger than in metals. As field penetrates deep inside the semiconductors it gets absorbed and the resulting effective loss in the doped semiconductors is actually larger than in metals [7].

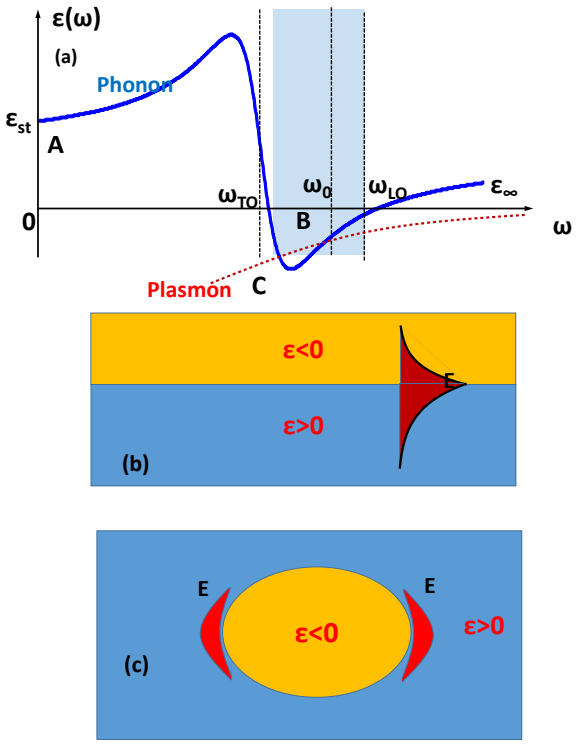

Fig. 2 (a) Dispersion of phonons and plasmons. (b) Propagating SphP; (c) Localized SPhP

But there exists yet another pathway leading to extensively low loss negative permittivity materials in the IR region – using the motion ions in place of free carriers [6]. Just like the oscillations of free carriers in metal or semiconductors, the collective oscillations of ions in polar dielectrics (commonly referred to as optical phonons) engender the oscillating space charges. These oscillations in turn can couple (hybridize) with the electro-magnetic field (photons) and the combined modes are known as phonon polaritons. The optical phonons are characterized by the (transverse optical phonon) resonance frequency $\omega_{TO}(\boldsymbol{k})$ (typically dependence on the wave vector $\boldsymbol{k}$ is rather weak) and the dispersion of the dielectric constant can be modeled by the Lorentzian oscillator,

$$\varepsilon_r(\omega) = \varepsilon_\infty \left(1 + \frac{\omega_P^2}{\omega_{TO}^2 - \omega^2 - j\omega\gamma}\right) \tag{9}$$

where ε_∞ is the high frequency (optical) dielectric constant of the material, γ is the damping rate, and the plasma $\omega_P^2 = Ne^{*2}/\varepsilon_0\varepsilon_\infty M_r$ where N is the density of polar bonds, e^* is their effective mass and M_r is the reduced mass. The real part of dielectric constant becomes equal to 0 at the frequency of $\omega_{LO} = \sqrt{\omega_{TO}^2 + \omega_P^2}$ called the frequency of longitudinal optical phonons. Now, as one can see from Fig.2a in the frequency range $\omega_{TO} < \omega < \omega_{LO}$ the real part of the dielectric constant is negative and the propagating electro-magnetic waves are not supported in this so-called Reststrahlen region, the

interface modes, called surface phonon-polariton (SPhP) do exist at the interface between two dielectrics, one with positive and one with negative dielectric constants as shown in Fig.2b where the propagating SPhP is shown and Fig.2c depicting the localized SPhP mode. Both the localized and propagating modes look every bit similar to their counterparts in the metal structures-surface plasmon polaritons (SPP's) which is not surprising given that the dispersion of metal looks similar,

$$\varepsilon_{met}(\omega) = \varepsilon_{\infty}\left(1 - \frac{\omega_p^2}{\omega^2 + j\omega\gamma}\right) \tag{10}$$

and can be obtained from (9) by simply setting the resonance frequency to zero. The dispersion of the metal is also shown (not necessary to scale) as a dotted line in Fig.2a

The most attractive feature of SPhPs, which has gave impetus to the whole new field of "phononics" is that the damping rate of optical phonons, caused by the anharmonicity, is typically as slow a a few picoseconds. This compares very favorably with the damping rate of SPP's, caused by the phonon and surface assisted absorption in the metal, which happens to be on the order of 10's of femtoseconds. Hence it seems logical that in the IR region the SPhPs should have multiple advantages over the SPP's in terms of the propagation length, lifetime and the field enhancement. Indeed, a significant amount of work in phononics had been performed in the course of the last decade and many of the plasmonic experiments previously performed in the visible range, have been successfully implemented in the Mid-IR region using phononic structures. Among them are

While the results clearly demonstrate that narrow resonances are indeed achievable in phononic structures, it is not clear that the degree of the field enhancement them is superior to what can be attained with metals, or doped semiconductors. The presence of the resonance frequency ω_{TO} in the denominator of (9) vs. the absence of it in (10) is expected to make the difference, but how big is this difference and what are the physical reasons for it has not been investigated in detail. In this work we present a simple and physically transparent theory that elucidates the difference between phononic and plasmonic materials using only the energy conservation considerations.

2.b Energy balance in polar dielectric structures

Let us consider the energy balance inside a mode contained within some volume of dielectric with relative permittivity $\varepsilon_r(\omega)$. If the characteristic dimension of the volume is a, then the electric field can be written as roughly $\boldsymbol{E}\sin(\pi x/a)\sin(\omega t)$ and magnetic field as $\boldsymbol{H}\cos(\pi x/a)\cos(\omega t)$. Then from the Maxwell's equation $\nabla\times\boldsymbol{H} = i\omega\varepsilon_0\varepsilon_r\boldsymbol{E}$ one can obtain the order-or-magnitude relation between the magnitudes of two fields,

$$H \approx \frac{\omega a}{\pi}\varepsilon_0\varepsilon_r E = \frac{2a}{\lambda}\frac{\varepsilon_r E}{\eta_0} \tag{11}$$

The time-averaged electric energy density can be written as

$$\langle U_E \rangle = \frac{1}{4}\varepsilon_0 \frac{\partial\left(\omega\varepsilon_r^{'}\right)}{\partial\omega}E^2 \tag{12}$$

where $\varepsilon_r^{'}$ is the real part of dielectric constant while the time-averaged magnetic energy density is

$$\langle U_M \rangle = \frac{1}{4}\mu_0 |H|^2 \sim \left(\frac{2na}{\lambda}\right)^2 \frac{1}{4}\varepsilon_0\varepsilon_r^{'}E^2 \tag{13}$$

where $n = \mathrm{Re}\left(\sqrt{\varepsilon_r}\right)$. If one considers the lowest order mode in the cavity, with $a = \lambda / 2n$ one immediately obtains the energy conservation relation $\int \langle U_E \rangle dV = \int \langle U_M \rangle dV$. But the time averaged picture does not properly represent the energy balance in the mode since the electric energy includes contributions oscillating 90 degrees out of phase with each other (in-phase and quadrature components). According to the Lorentz oscillator model, used to derive (9) the relative displacement of ions is

$$x(t) = \frac{e^* / M_r}{\left[\left(\omega_{TO}^2 - \omega^2\right)^2 + \omega^2\gamma^2\right]^{1/2}} E\sin(\omega t - \varphi) \tag{14}$$

where $\tan\varphi = \gamma^2\omega^2(\omega_{TO}^2 - \omega^2)$

and the velocity of this motion is

$$\dot{x}(t) = -\omega\frac{e^* / M_r}{\left[\left(\omega_{TO}^2 - \omega^2\right)^2 + \omega^2\gamma^2\right]^{1/2}} E\cos(\omega t - \varphi) \tag{15}$$

Then we obtain the expressions for the kinetic

$$U_K(t) = \frac{1}{2}NM_r\dot{x}^2(t) = \frac{1}{2}\frac{\omega^2\omega_P^2}{\left(\omega_{TO}^2 - \omega^2\right)^2 + \omega^2\gamma^2}\varepsilon_0\varepsilon_\infty E^2\cos^2(\omega t - \varphi) \tag{16}$$

and potential

$$U_P(t) = \frac{1}{2}NM_r\omega_{TO}^2 x^2(t) = \frac{1}{2}\frac{\omega_{TO}^2\omega_P^2}{\left(\omega_{TO}^2 - \omega^2\right)^2 + \omega^2\gamma^2}\varepsilon_0\varepsilon_\infty E^2\sin^2(\omega t - \varphi) \tag{17}$$

energy densities inside the volume. The potential energy can be split into two parts as

$$U_P(t) = \frac{1}{2}\frac{\omega_P^2(\omega_{TO}^2 - \omega^2 + \omega^2)}{\left(\omega_{TO}^2 - \omega^2\right)^2 + \omega^2\gamma^2}\varepsilon_0\varepsilon_\infty E^2\sin^2(\omega t) = U_{P1}(t) + U_{P2}(t) \tag{18}$$

The first part is

$$U_{P1}(t)=\frac{1}{2}\frac{\omega_P^2(\omega_{TO}^2-\omega^2)}{\left(\omega_{TO}^2-\omega^2\right)^2+\omega^2\gamma^2}\varepsilon_0\varepsilon_\infty E^2\sin^2(\omega t-\varphi)=\frac{1}{2}\varepsilon_0\left(\varepsilon_r^{'}-\varepsilon_\infty\right)E^2\sin^2(\omega t-\varphi) \tag{19}$$

where $\varepsilon_r^{'}$ is the real part of the dielectric constant (9) and the second part

$$U_{P2}(t)=\frac{1}{2}\frac{\omega^2\omega_P^2}{\left(\omega_{TO}^2-\omega^2\right)^2+\omega^2\gamma^2}\varepsilon_0\varepsilon_\infty E^2\sin^2(\omega t-\varphi)=\frac{1}{4}\varepsilon_0\omega\frac{\partial\varepsilon_r^{'}}{\partial\omega}E^2\sin^2(\omega t-\varphi) \tag{20}$$

has the same amplitude as kinetic energy (16) but with a 90 phase shift. The total energy density can then be found as

$$U_E(t)=U_{P1}(t)+U_{P2}(t)+U_\infty(t)+U_K(t)=\frac{1}{2}\varepsilon_0\varepsilon_r^{'}E^2\sin^2(\omega t-\varphi)+\frac{1}{4}\varepsilon_0\omega\frac{\partial\varepsilon_r^{'}}{\partial\omega}E^2[\sin^2(\omega t-\varphi)+\cos^2(\omega t-\varphi)]=$$

$$=\frac{1}{2}\varepsilon_0\varepsilon_r^{'}E^2\sin^2(\omega t-\varphi)+\frac{1}{4}\varepsilon_0\omega\frac{\partial\varepsilon_r^{'}}{\partial\omega}E^2 \tag{21}$$

where

$$U_\infty(t)=\frac{1}{2}\varepsilon_0\varepsilon_\infty E^2\sin^2(\omega t)\approx\frac{1}{2}\varepsilon_0\varepsilon_\infty E^2\sin^2(\omega t-\varphi) \tag{22}$$

is the sum of energy stored in the electric field proper, $U_{EF}=\frac{1}{2}\varepsilon_0E^2$ and the potential energy associated with oscillations of valence electrons, $U_V=\frac{1}{2}\varepsilon_0(\varepsilon_\infty-1)E^2$ Neglecting a small phase shift φ in (22)amounts to the error on the scale of γ^2/ω_p^2 .Averaging (21) over the time immediately leads to (12).

Now we can see that the energy oscillating roughly in phase (i.e. as $\sin^2(\omega t-\varphi)$) with the electric field, which can be referred to as either “in phase” or “potential” is

$$U_I(t)=U_\infty(t)+U_{P1}(t)+U_{P2}(t) \tag{23}$$

and has three components The first of them, $U_\infty(t)$ is entirely static as it has no frequency dependence. The second component, $U_{P1}(t)$ is only weakly resonant and dominates the frequency response in the normal dispersion region. The third component, $U_{P2}(t)$, whose amplitude is equal to the amplitude of kinetic energy $U_K(t)$ is very dispersive and becomes the dominant factor in the anomalous dispersion region.

The energy that oscillates roughly 90 degrees out of phase with the electric field (i.e. as $\cos^2(\omega t-\varphi)$) can be referred to as either “quadrature” or “kinetic”

$$U_Q(t)=U_K(t)+U_M(t) \tag{24}$$

and has two components, the actual kinetic energy of ions $U_K(t)$ which is strongly dispersive and the magnetic energy $U_M(t)$. Whether kinetic of magnetic energy dominates depends on the dimensions of the mode. Comparing (16) with (13) immediately yields

$$\frac{U_K}{U_M} \sim \left(\frac{\lambda}{2a}\right)^2 \frac{\omega}{2\left|\varepsilon_r^{'}\right|^2}\frac{\partial \varepsilon_r^{'}}{\partial \omega} \sim \frac{1}{2}\left(\frac{\lambda}{2a}\right)^2 \left(\frac{\omega^2}{\varepsilon_\infty \omega_P^2}\right) \sim \frac{1}{2}\left(\frac{\lambda_P}{2an_\infty}\right)^2 \tag{25}$$

This is the most interesting result indicating that the ratio of two energies depends only on the size of the mode relative to the plasma wavelength.

Now, the self-sustaining eigenmodes can exist only when the in-phase and quadrature energies are equal to each other, i.e. $\int \langle U_I(t)\rangle d^3\boldsymbol{r} = \int \langle U_Q(t)\rangle d^3\boldsymbol{r}$ or

$$\frac{1}{4}\int \varepsilon_r^{'} E^2(\boldsymbol{r}) d^3r + \frac{1}{8}\omega \int \frac{\partial \varepsilon_r^{'}}{\partial \omega} E^2(\boldsymbol{r}) d^3r = \frac{1}{8}\omega \int \frac{\partial \varepsilon_r^{'}}{\partial \omega} E^2(\boldsymbol{r}) d^3r + \left(\frac{2na}{\lambda}\right)^2 \frac{1}{4}\int \varepsilon_r^{'} E^2(\boldsymbol{r}) d^3r \tag{26}$$

Note that we have kept two equal dispersive terms on both sides of (26) in order to obtain the solutions from the energy balance considerations. Clearly, there exist two possible solutions of (26) that do not depend on the dimensions of the mode and field obviously occur when the dielectric constant is zero, or when dispersive terms on both sides approach the infinity. The first solution occurs at $\omega = \omega_{LO}$ and is nothing but the (bulk) longitudinal optical phonon. The second solution occurs at $\omega = \omega_{TO}$ and is obviously a transverse optical phonon mode. Neither one of these solutions are interesting from the practical point of view. In the TO mode the electric field is zero and the electric field inside the LO phonon mode is all contained deep inside the material. Another solution, occurring when $a \sim \lambda / 2n$ is obviously a standard mode inside the dielectric resonator (as shown in the Fig.3a), but if the spatial extent of the mode is sub-wavelength, which in context of this work means $a << \lambda / 2n$ the only way the solution is attainable is when the medium is spatially inhomogeneous and incorporates the regions with both negative and positive dielectric constants so that $\int \varepsilon_r^{'} E^2(\boldsymbol{r}) d^3r \approx 0$. The easiest ways in which it can be accomplished is using a sub-wavelength object made from a dielectric in the Reststrahlen region $\varepsilon_r^{'}(\omega) < 0$ surrounded by the cladding made from a "normal" or low-dispersion dielectric with $\varepsilon_{r,cl}^{'}(\omega) > 0$, as shown in Fig.3b Whenever the energy balance condition (26) is satisfied at frequency ω_0 this frequency is the eigen-frequency of the SPhP mode. Also shown in Fig.3c is the sub-wavelength SPP structure made from the doped semiconductor.

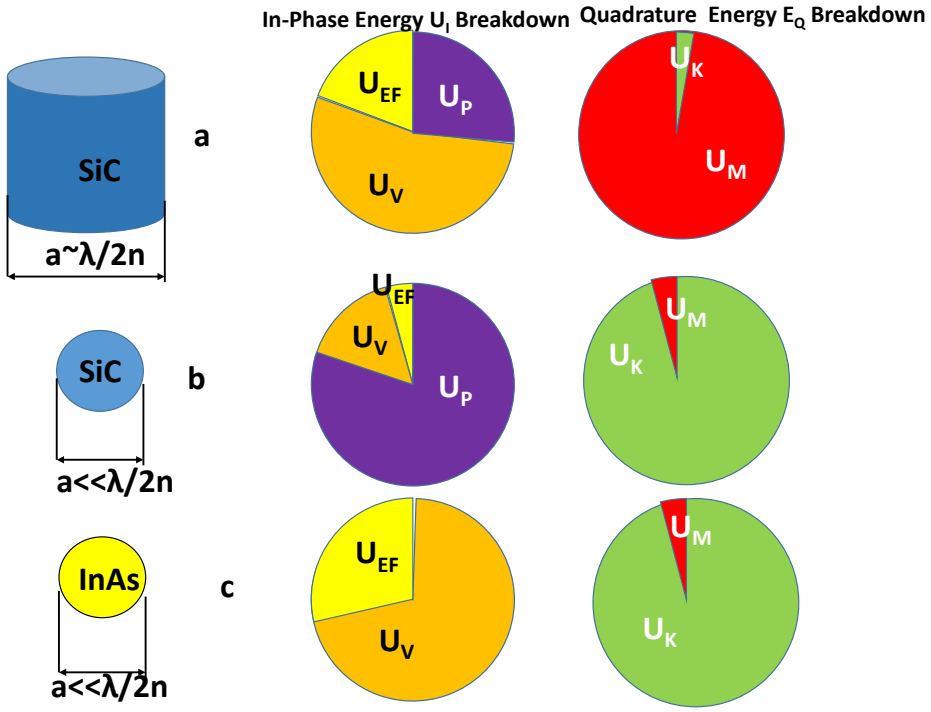

Fig.3 The breakdown of energies in three different resonant structures in mid-IR region (a) dielectric resonator (b)localized surface phonon polariton (c0 localized surface plasmon polariton

Next to each structure we show the breakdown of in-phase U_I and quadrature U_Q energies. For the typical dielectric resonator operated outside the Reststrahlen (Fig 3a) region the in-phase energy is split between the energies of electric field U_{EF} , valence electrons U_V and potential energy of ions U_P. For the sub-wavelength SPhP (Fig.3b) the potential energy of ions dominates, but in the SPP shown in Fig.3c this potential energy is absent since free carriers by definition have no potential energy. This dominance vs absence of potential energy of ions constitutes the major difference between SPhPs and SPPs with the repercussions illustrated below. As far as the quadrature component of energy goes, SPhP and SPP behave similarly, with kinetic energy of ions or electrons U_K dominating the magnetic energy U_M in stark constant to the dielectric resonator of Fig.3a. energy breakdown shown above it.

2.c Localized Surface Phonon Polaritons –enhancing energy and electric field

To illustrate this, consider a spherical particle with a radius *a* and real $\varepsilon_r(\omega)$ placed in the cladding as shown in Fig.2c with a dipole moment $\boldsymbol{p} = p\hat{\boldsymbol{z}}$ that is related to the field inside it as

$$\boldsymbol{p} = \frac{4}{3}\pi a^3 \varepsilon_0 \left(\varepsilon_r - \varepsilon_{r,cl}\right) \boldsymbol{E}_{in} \tag{27}$$

The field outside the particle is

$$\boldsymbol{E}_{out}(\boldsymbol{r}) = \frac{1}{4\pi\varepsilon_0 \varepsilon_{r,cl} r^3}\left[3\left(\boldsymbol{p}\cdot\hat{\boldsymbol{r}}\right)\hat{\boldsymbol{r}} - \boldsymbol{p}\right] = \left|E_{in}\right|\frac{a^3}{r^3}\frac{\varepsilon_r - \varepsilon_{r,cl}}{3\varepsilon_{r,cl}}\left[3\cos\theta(\hat{\boldsymbol{z}}\cos\theta + \hat{\boldsymbol{r}}_\perp \sin\theta) - \hat{\boldsymbol{z}}\right] \tag{28}$$

where $\hat{\boldsymbol{r}}_\perp$ is the unit vector in the *xy* plane. Then we evaluate the energy integral outside as

$$I_{out} = \varepsilon_{r,cl}\int \left|E_{out}(r,\theta)\right|^2 d^3\boldsymbol{r} = 2\pi\varepsilon_{r,cl}\left|E_{in}\right|^2 \varepsilon_{r,cl}\left[\frac{\varepsilon_r - \varepsilon_{r,cl}}{3\varepsilon_{r,cl}}\right]^2 \int_a^\infty \frac{a^6 r^2 dr}{r^6}\int_0^\pi (3\cos^2\theta + 1) d\cos\theta =$$

$$= \frac{8}{3}\pi a^3 \varepsilon_{r,cl}\left[\frac{\varepsilon_r - \varepsilon_{r,cl}}{3\varepsilon_{r,cl}}\right]^2 \left|E_{in}\right|^2 \tag{29}$$

and the energy interval inside is obviously

$$I_{in} = \int \varepsilon_r \left|E_{in}(r,\theta)\right|^2 d^3\boldsymbol{r} = \frac{4}{3}\pi a^3 \varepsilon_r \left|E_{in}\right|^2 \tag{30}$$

Which immediately leads us to the condition

$$I_{in} + I_{out} = \varepsilon_r + 2\varepsilon_{r,cl}\left[\frac{\varepsilon_r - \varepsilon_{r,cl}}{3\varepsilon_{r,cl}}\right]^2 = 0 \tag{31}$$

Obviously the solution for the dipole mode $\varepsilon_r(\omega) = -2\varepsilon_{r,cl}$ satisfies (31) and the SPhP eigen frequency is

$$\omega_0^2 = \omega_{TO}^2 + \omega_P^2 / (1 + 2\varepsilon_{r,cl}/\varepsilon_\infty) \tag{32}$$

Interestingly enough, the second solution of (31) is $2\varepsilon_r(\omega) = -\varepsilon_{cl}$ corresponds to the eigenmode of the spherical void inside the metal that is filled with a dielectric.

One can therefore make an important statement regarding the energy balance in the deeply subwavelength SPhP (and also, of course, SPP) mode. Equation (26) can be re-written as

$$\int \langle U_{P2}\rangle d^3\boldsymbol{r} = \int \langle U_K\rangle d^3\boldsymbol{r} = \frac{1}{8}\omega\int \frac{\partial\varepsilon_r'}{\partial\omega} E_{in}^2(\boldsymbol{r}) d^3 r \tag{33}$$

Indicating that the energy in the mode oscillates between the kinetic energy inside the dispersive medium and the combination of the potential energy of ions and electrons. The total energy can then be estimated simply as

$$\int \langle U_E \rangle d^3\mathbf{r} = 2\int \langle U_K \rangle d^3\mathbf{r} = \frac{1}{4}\omega \int \frac{\partial \varepsilon_r^{'}}{\partial \omega} E_{in}^2(\mathbf{r}) d^3 r = \frac{1}{3}\pi a^3 \varepsilon_0 \omega \frac{\partial \varepsilon_r^{'}}{\partial \omega} E_{in}^2 = \frac{2}{3}\pi a^3 \varepsilon_0 \varepsilon_\infty \frac{\omega^2 \omega_P^2}{\left(\omega_{TO}^2 - \omega^2\right)^2 + \omega^2 \gamma^2} E_{in}^2 \quad (34)$$

Substituting the eigen frequency from (32) and using the fact that $\omega_P >> \gamma$ we obtain

$$\int \langle U_E \rangle d^3\mathbf{r} = \frac{2}{3}\pi a^3 \varepsilon_0 \left(\varepsilon_\infty + 2\varepsilon_{r,cl}\right)\left[1 + \frac{\omega_{TO}^2}{\omega_P^2}\left(1 + 2\varepsilon_{r,cl}/\varepsilon_\infty\right)\right] E_{in}^2 = \frac{2}{3}\pi a^3 \varepsilon_0 \left(\varepsilon_\infty + 2\varepsilon_{r,cl}\right) K_{ph} E_{in}^2, \quad (35)$$

where the factor describing the "excess" potential energy stored in the oscillations of atoms and electrons is

$$K_{ph} = 1 + \frac{\omega_{TO}^2}{\omega_P^2}\left(1 + 2\varepsilon_{r,cl}/\varepsilon_\infty\right) = \frac{\varepsilon_{st} + 2\varepsilon_{r,cl}}{\varepsilon_{st} - \varepsilon_\infty} \quad (36)$$

and ε_{st} is the static dielectric constant. Using (32) one can also express the "excess potential energy factor" as

$$K_{ph} = \frac{\omega_0^2}{\omega_P^2}\left(1 + 2\varepsilon_{r,cl}/\varepsilon_\infty\right) \quad (37)$$

Obviously, for the surface plasmon polariton this factor is equal to unity, but for a typical phononic medium, such as SiC with $\varepsilon_{st} = 9.7$ and $\varepsilon_\infty = 6.7$ and dielectric cladding with $\varepsilon_{r,cl} = 1$ one obtains $K_{ph} \sim 4$

Let us now consider the field and energy enhancement attainable with the SPhP using the same spherical nanoparticle model. To do this we shall first find the effective volume which we define as

$$V_{eff} = \frac{\int \langle U_E \rangle d^3\mathbf{r}}{\frac{1}{4}\varepsilon_0 \varepsilon_{r,cl} \left|E_{\max}\right|^2} = \frac{2}{3}\pi a^3 \left(\frac{\varepsilon_\infty}{\varepsilon_{r,cl}} + 2\right) K_{ph} = V_n \left(1 + \frac{\varepsilon_\infty}{2\varepsilon_{r,cl}}\right) K_{ph} = \frac{3}{2} V_n K_{env} K_{ph} \quad (38)$$

where the maximum field is $E_{\max} = 2E_{in}$ and $V_n = 4/3\pi a^3$ is the nanoparticle volume. The term in the parenthesis indicates that a significant part of energy is stored in the oscillation of valence electrons, and the second term K_{ph} indicates that even larger fraction of energy is stored in the lattice vibration. As a result, even when the **energy** can be efficiently concentrated by the nanoparticle, the enhancement of the **electric field** may be less than stellar.

We now turn our attention to the estimates of the enhancement. In the presence of the external electric field $\boldsymbol{E}_{ext}$ the nanoparticle acquires the dipole moment

$$\boldsymbol{p}_\omega = 4\pi\varepsilon_0 \varepsilon_{cl} a^3 \boldsymbol{E}_{ext} \frac{\varepsilon_r - \varepsilon_{r,cl}}{\varepsilon_r + 2\varepsilon_{r,cl}} \quad (39)$$

Substituting (9) we obtain in the vicinity of resonance $\omega \approx \omega_0$ (32)

$$\boldsymbol{p} = 4\pi\varepsilon_0\varepsilon_{cl}a^3\frac{\omega_0^2 - 3\omega_{TO}^2\dfrac{\varepsilon_{cl}/\varepsilon_\infty}{1+2\varepsilon_{cl}/\varepsilon_\infty} - \dfrac{1-\varepsilon_{r,cl}/\varepsilon_\infty}{1+2\varepsilon_{r,cl}/\varepsilon_\infty}\omega^2}{\omega_0^2 - \omega^2 - j\omega\gamma}\boldsymbol{E}_{ext} \approx 4\pi\varepsilon_0\varepsilon_{cl}^2a^3\frac{3}{\varepsilon_\infty + 2\varepsilon_{cl}}\frac{\omega_0^2 - \omega_{TO}^2}{\omega_0^2 - \omega^2 - j\omega\gamma}\boldsymbol{E}_{ext} =$$

$$= 4\pi\varepsilon_0\varepsilon_{cl}^2\varepsilon_\infty a^3\frac{3}{\left(\varepsilon_\infty + 2\varepsilon_{cl}\right)^2}\frac{\omega_P^2}{\omega_0^2 - \omega^2 - j\omega\gamma}\boldsymbol{E}_{ext} \tag{40}$$

According to (28)

$$\boldsymbol{E}_{\max} = \frac{\boldsymbol{p}}{2\pi\varepsilon_0\varepsilon_{r,cl}a^3} = \varepsilon_{cl}\varepsilon_\infty\frac{6}{\left(\varepsilon_\infty + 2\varepsilon_{cl}\right)^2}\frac{\omega_P^2}{\omega_0^2 - \omega^2 - j\omega\gamma}\boldsymbol{E}_{ext} \tag{41}$$

Now, if we introduce quality factor $Q_0 = \omega_0/\gamma$ then at resonance we obtain

$$\boldsymbol{E}_{\max} = \varepsilon_{r,cl}\varepsilon_\infty\frac{6}{\left(\varepsilon_\infty + 2\varepsilon_{cl}\right)^2}\frac{\omega_P^2}{\omega_0^2}Q_0\boldsymbol{E}_{ext} = \frac{6}{\varepsilon_\infty/\varepsilon_{r,cl} + 2}\frac{Q_0}{K_{ph}}\boldsymbol{E}_{ext} = \frac{E_{\max,0}}{K_{env}K_{ph}}\boldsymbol{E}_{ext} \tag{42}$$

where $E_{\max,0} = 2Q_0E_{ext}$ is the enhancement achieved near the nanosphere made from a "classical Drude" metal with $\varepsilon_\infty = 1$ placed into the vacuum $\varepsilon_{r,cl} = 1$ and $K_{env} = (\varepsilon_\infty/\varepsilon_{r,cl} + 2)/3$ is the "deviation" from that picture. This factor is typically close to unity in both SPP and SPhP and it is the "excess potential energy" factor

As one can see, the same two factors are responsible for the decrease in the enhancement of the field. Now we can use (38) and (42) to find the energy inside the SPhP mode

$$\int\langle U_E\rangle d^3\boldsymbol{r} = \frac{1}{4}\varepsilon_0\varepsilon_{r,cl}E_{\max}^2V_{eff} = \frac{1}{4}\varepsilon_0\varepsilon_{r,cl}V_n\left(1+\frac{\varepsilon_\infty}{2\varepsilon_{r,cl}}\right)K_{ph}\left(\frac{6}{\varepsilon_\infty/\varepsilon_{r,cl}+2}\right)^2\left(\frac{Q_0}{K_{ph}}\right)^2E_{ext}^2 =$$

$$= \frac{9}{2}V_n\frac{Q_0^2}{\left(1+\dfrac{\varepsilon_\infty}{2\varepsilon_{r,cl}}\right)K_{ph}}\langle U_{ext}\rangle = 3V_n\frac{Q_0^2}{K_{env}K_{ph}}\langle U_{ext}\rangle \tag{43}$$

So, here is what happens – first of all, the dipole in phononic nanoparticle is less by the factor $K_{env}K_{ph}$ and then the effective volume is larger by the same factor – hence the *energy density* gets enhanced by a factor $(K_{env}K_{ph})^2$ less.

It is also interesting to see by how much one can enhance the spontaneous emission rate γ_0. The Purcell factor that describes enhancement relative to that into the mode in an infinite dielectric can be found as

$$F_P = \frac{3}{4\pi}\left(\frac{\lambda}{n_{cl}}\right)^3 V_{eff}^{-1}\frac{\omega}{\gamma_R+\gamma} = \frac{2}{3\pi}\left(\frac{\lambda}{n_{cl}}\right)^3 \frac{V_n^{-1}}{K_{env}K_{ph}}\frac{\omega}{\gamma_R+\gamma} \tag{44}$$

The radiative decay of the dipole (27) in turn can be found as

$$\gamma_R = 4\pi^2 \frac{V_n}{K_{env}K_{ph}}\left(\frac{n_{cl}}{\lambda}\right)^3 \omega \tag{45}$$

If we introduce the "scaled" volume of nanoparticle as $V_n^{'} = V_n(n_{cl}/\lambda^3)$ and take into account that only the fraction $\gamma_R/(\gamma_R+\gamma)$ of radiation emitted into the SPhP mode radiates outside we obtain for the effective enhancement factor

$$F_{P,eff} = \frac{8\pi}{3}\frac{1}{\left(K_{env}K_{ph}\right)^2}\frac{1}{\left(4\pi^2\frac{V_n}{K_{env}K_{ph}}\right)^2+\frac{1}{Q_0^2}} \le \frac{8\pi}{3}\frac{Q_0^2}{\left(K_{env}K_{ph}\right)^2} \tag{46}$$

This is precisely the same result as the one for the field enhancement. On should note that typically the Q-factor for SiC is on the scale of 200 or so vs.40 -50 for InAs. Therefore, both field enhancement and Purcell factor characteristics in SPhP's and SPP's operating in mid IR region are roughly comparable, despite nearly order of magnitude longer scattering times for phonons.

2.d Propagating Surface Phonon Polaritons

Let us now consider a propagating polariton between two media one with real positive dielectric constant with weak dispersion $\varepsilon_{r,cl}$ and one with the dispersive complex dialectic constant $\varepsilon_r(\omega)$ corresponding to either phononic (9) or plasmonic (10) material. The dispersion of the propagation constant of the polariton at the interface is

$$\beta^2(\omega) = k_{cl}^2(\omega)\frac{\varepsilon_r(\omega)}{\varepsilon_r(\omega)+\varepsilon_{r,cl}} \tag{47}$$

where $k_{cl}^2(\omega) = \varepsilon_{r,cl}^{1/2}\omega / c$. Differentiating (47) over frequency and assuming that one operates near the resonance, i.e. $\varepsilon_r^{'}(\omega) \approx -\varepsilon_{r,cl}$, one can obtain the expression for the group velocity

$$v_g^{-1} = \frac{d\beta}{d\omega} = \frac{\beta^3}{2k_{cl}^2\varepsilon_{r,cl}}\frac{\partial\varepsilon_r^{'}}{\partial\omega} \approx \frac{\beta^3}{k_{cl}^2\varepsilon_{r,cl}}\frac{\omega\omega_P^2}{\left(\omega_{TO}^2-\omega^2\right)^2} = \frac{\beta^3}{\omega k_{cl}^2\varepsilon_{r,cl}}\frac{\omega^2\omega_P^2}{\left(\omega_{TO}^2-\omega^2\right)^2} \approx \frac{1}{v_{cl}}\frac{\beta^3}{k_{cl}^3}\left(\frac{1}{\varepsilon_{r,cl}}+\frac{1}{\varepsilon_\infty}\right)K_{ph}^{'} \qquad (48)$$

where v_{cl} is the propagation velocity in cladding. As expected, the group velocity in the SPhP is reduced by an additional factor of K_{ph} when compared to the SPP because most of the energy is not associated with the photon but with the lattice vibrations. Note that the factor β^3 / k_{cl}^3 is associated both with the reduction of magnetic field and with the fact that the Poynting vector inside the negative permittivity medium is directed backward.

Also from (47) we can obtain the expression for the imaginary part of propagation function

$$\beta^{"} = \frac{\beta^3}{2k_{cl}^2\varepsilon_{r,cl}}\varepsilon_r^{"} \approx \frac{\beta^3}{k_{cl}^2\varepsilon_{r,cl}}\frac{\omega\omega_P^2\gamma}{\left(\omega_{TO}^2-\omega^2\right)^2} = \frac{1}{2}\gamma v_g^{-1} \qquad (49)$$

It means that the propagation length of the SPhP is

$$L_p = 1/2\beta^{"} = v_g/\gamma \simeq \left(\lambda_{cl}/2\pi\right)(k_{cl}/\beta)^3 Q_0 / K_{ph}^{'} \qquad (50)$$

Once again, the factor Q_0 / K_{ph} presents itself, indicating that enhancement of the propagation length in SPhP is small relative to SPP, despite lower scattering rate.

2.e. Conclusions

Using a simple energy balance model we have shown that although the scattering rate of optical phonons in polar dielectrics is order-of-magnitude less than scattering rate of electrons in doped semiconductors and two orders of magnitude less than in metals, this advantage is counter-balanced by the smaller effective plasma frequency and the fact that significant part for energy is stored in the potential energy of lattice vibrations. Therefore, phononics, while being a valuable technology is not expected to fully supplant metal plasmonics even in the long wavelength region of the spectrum.

3. Study of the effect of Landau damping on maximum field enhancement attainable with the plasmonic dimers and nanoantennas

We show that Landau damping presents the most practically-relevant limit to the achievable plasmonic enhancement inside the narrow gaps of plasmonic dimers and other similarly-shaped plasmonic nanoantennas..

The most remarkable feature of plasmonic structures in the optical range is their ability to concentrate the optical field into the surface plasmon polariton (SPP) modes with volumes that can be orders of magnitude less than $(\lambda/2n)3$ where λ is the wavelength in vacuum and n is the refractive index. If the SPP mode can be coupled to the propagating electro-magnetic waves, the peak field inside the mode can be enhanced by orders of magnitude relative to the incident wave. In such structures, called (plasmonic) nanoantennas, all the linear and especially nonlinear processes get enhanced [8, 9]. Typical nanoantenna incorporates a dielectric gap between two metallic structures of various geometry and it is in this gap where the concentrated electric field gets enhanced. A suitable example of a nanoantenna is a plasmonic dimer (Fig. 4a) consisting of two metal spheres or radius a separated by a dielectric gap d into which the object of the plasmonic enhancement (an atom, a molecule or a quantum dot) is placed. Naturally, reduction of the gap size causes decrease in the SPP volume which is expected to be accompanied by the commensurate increase in the energy density of the SPP field and Purcell factor. However, once the gap size decreases to a few nanometers and less, both the field enhancement and Purcell factor cease to increase while the linewidth of the resonance eventually broadens to the degree where the SPP resonances are no longer discernible [10]. Hence the size of the gap always needs to be optimized in order to attain maximum enhancement of a given process.

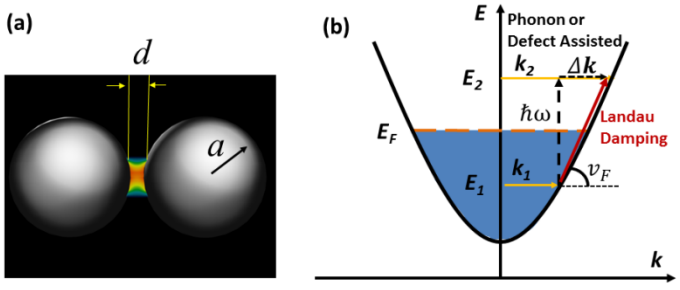

Fig. 4. (a) Illustration of the SPP field concentration in plasmonic dimer and (b) origin of Landau Damping – direct transition between two states with different wave-vectors k_1 and k_2.

The reason for the "saturation" and eventual decline of the enhancement in the gap is the result of the Landau damping (LD) in the vicinity of the Fermi level in the metal (Fig. 4b) where direct transition between two electronic states below (k_1) and (k_2)above the Fermi level is allowed when the power spectrum of the SPP inside of metal contains wavevector components $k \geq \Delta k = k_2 - k_1$. Such components increase significantly with the tightening of the field confinement as the dimer radius and gap shrink. Conceptually, LD is equivalent to the phenomenologically described surface collision damping [11], since it the sharp boundary between conductor and dielectric that supplies large k-vector components required for LD. Figure 5 shows the dramatic impact of LD on both the shape and magnitude of the field in the SPP mode of the same silver and gold dimers of radius $a = 2.5$ nm and gap $d = 0.5$ nm. The field enhancement in the absence of LD for silver reaches 800 (Fig. 5a) but once the LD is taken into account it gets reduced by nearly two orders of magnitude (Fig. 5b). A comparable field enhancement reduction occurs in a gold dimer as shown in Fig. 5c and 5d. The dramatic decline of the field enhancement is the direct result of LD. In Fig. 6a and 6c one can see how the total damping including Landau and bulk damping (solid lines) grows as the gap gets narrow for a silver or gold dimer of various nanospheres sizes while the bulk damping (dashed line) remains unchanged. Figure 6b and 6d show their effective volume, a measure of field confinement, gets smaller as the gap narrows, but when LD is considered, it does not decrease as much, indicating the mode gets "squeezed out" of the gap and the plasmonic enhancement reaches its limit.

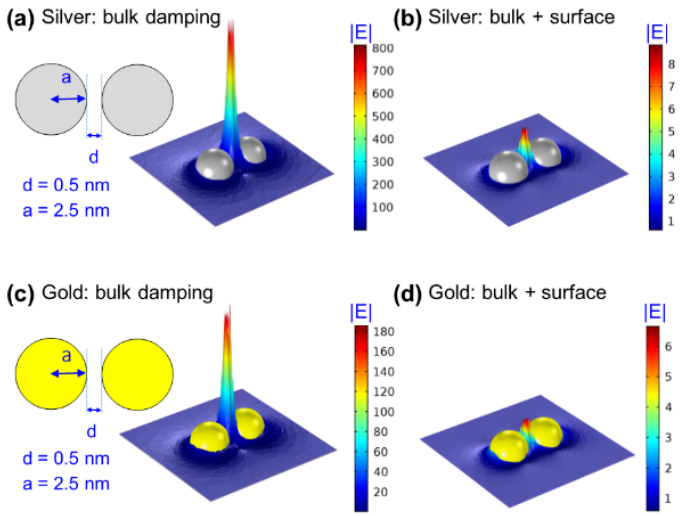

Fig. 5. SPP Field distribution in the silver dimer (a=2.5 nm and d=0.5 nm) taking into account (a) only bulk damping and (b) both bulk and surface damping, and corresponding results for the gold dimer of equal dimensions in (c) and (d).

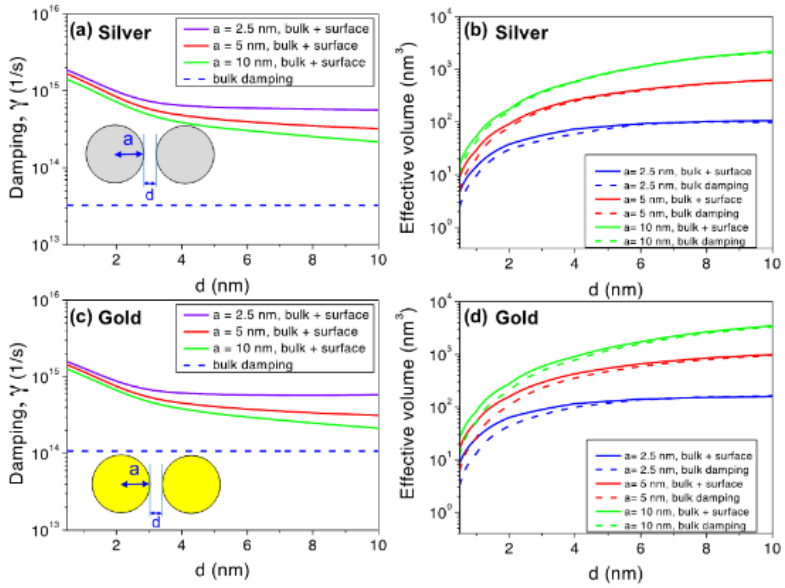

Fig. 6. (a) Total damping (solid lines) in the silver dimer as a function of gap width for three different radii compared with bulk damping (dashed line). (b) Effective mode volume as a function of gap width with (solid lines) and without (dashed lines) surface collisions. Corresponding results for the gold dimer in (c) and (d).

Let us now examine the maximum achievable optical field enhancement in the gap of either silver or gold dimer and reveal the impact of LD (surface collision) as the gap shrinks. One can see in Fig. 4 that for a silver or gold dimer of any radius the maximum enhancement grows rapidly with the decrease of the gap size when only bulk damping is accounted for (dashed curves), although the degree of enhancement varies for dimers of different sizes as explained in [12, 13]. However, once the LD is taken into account, the increase of enhancement is quite modest The largest actually occurs for a dimer with larger nanospheres ($a = 50$ nm) of greater effective mode volume, suggesting that greater enhancement is achieved when the SPP field spreads out more inside of the metal rather than being tightly bunched near the metal boundary – casing strong LD.

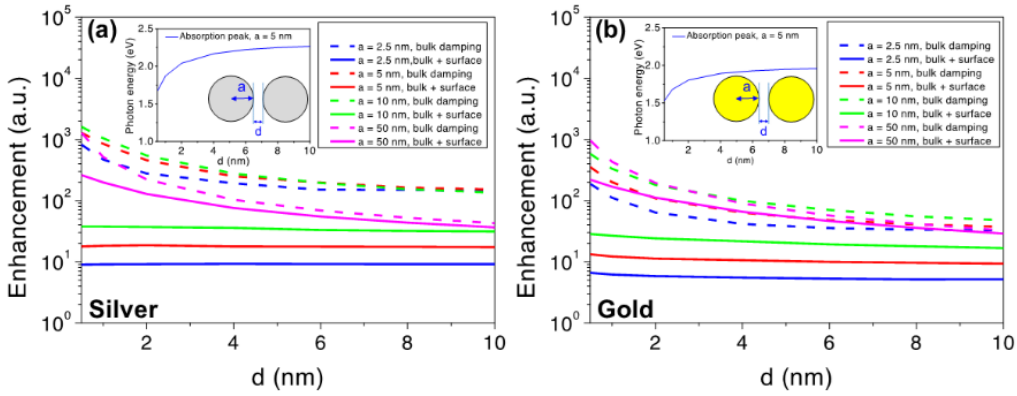

Fig. 7. Maximum enhancement as a function of gap width in (a) silver and (b) gold dimers of four different radii with (solid lines) and without (dashed lines) LD.

In conclusion, we have shown that LD (surface collisions) is the ultimate factor limiting the field enhancement and Purcell factors in metal dimers and similar structures.

4. Investigation of the possibility of creating a chemically stable lossless metal with Van-der-Waals materials.

In 2010 in our important work [14] we have predicted the existence of the so-called “lossless” metals The ideal “lossless” material should have an isolated partially filled conduction band separated by bandgaps from both valence and higher lying empty conduction bands, as shown in Fig.2 It is important to understand the difference between the proposed material and the more conventional highly doped semiconductors, such as III-V materials [, or conductive oxides .

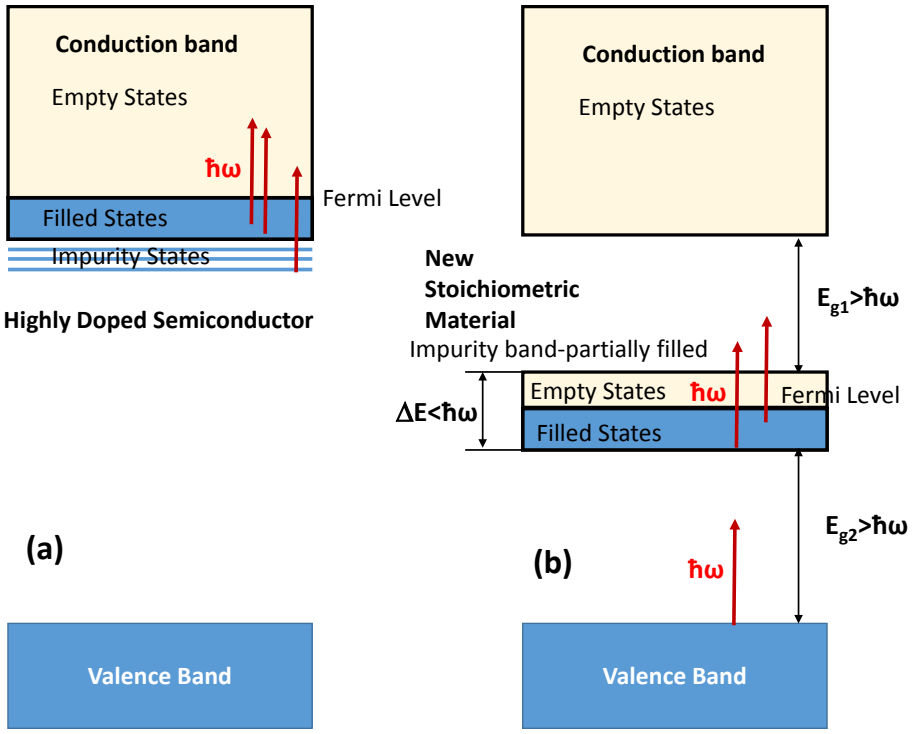

Fig.8 (a) Highly doped semiconductor with strong absorption. (b) Novel stoichiometric material that exhibits no absorption in a range of frequencies that are too high for the intraband absorption and too low for the interband absorption.

The band structure of a typical conductive oxide is shown in Fig.8a and is characterized by the broad **shallow impurity band** comprising the donors (for example Al substituting for donors in ZnO). The impurity band is essentially merged with the conduction band. If one now considers absorption of a photon (or plasmon-polariton) with energy $\hbar\omega$, there are plenty of empty states in the conduction band into which absorption can take place.

In contrast to this, the "lossless metal" of Fig.8b is characterized by **deep impurity levels** that are arranged stoichiometrically and form a deep impurity band that is half-full. Now, if the impurity band width ΔE is less than photon energy, while the bandgaps separating it from the conduction and valence bands, E_{g1} and E_{g2} respectively are larger than the photon energy $\hbar\omega$, the absorption is prohibited by energy conservation and the "metal" becomes transparent.

Now, upon exhaustive literature search we have identified that such structures can indeed exist. In this work we relied on Density functional calculations performed by the group of Prof. Thygesen that will be reported in the upcoming work in Nature Communications. They have

shown that Ohmic losses are reduced in certain layered metals, such as the transition metal dichalcogenide TaS2, due to an extraordinarily small density of states for scattering in the near-IR originating from their special electronic band structure. Based on this observation they proposed a new class of band structure engineered van der Waals layered metals composed of hexagonal transition metal chalcogenide-halide layers with greatly suppressed intrinsic losses. Using first principle calculations they show that the suppression of optical losses lead to improved performance for thin film wave guiding and transformation optics.

An example of such material, 1T-$AlCl_2$ is shown in Fig. 9 – clearly one can see the intermediate band which is half-filled and separated from the main valence and conductions bands.

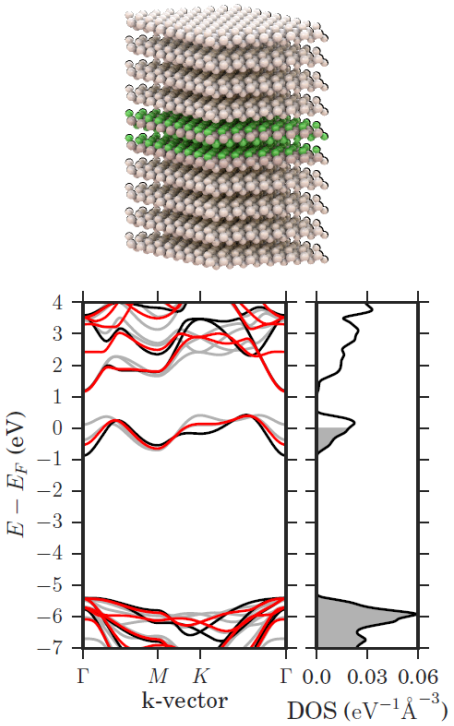

Fig.9 A low loss material T-AlCl2 (top) crystalline layered structure (bottom) Band structure

This observation is confirmed by calculation of the absorption in the AlCl2 and comparing it with silver in Fig.10 .

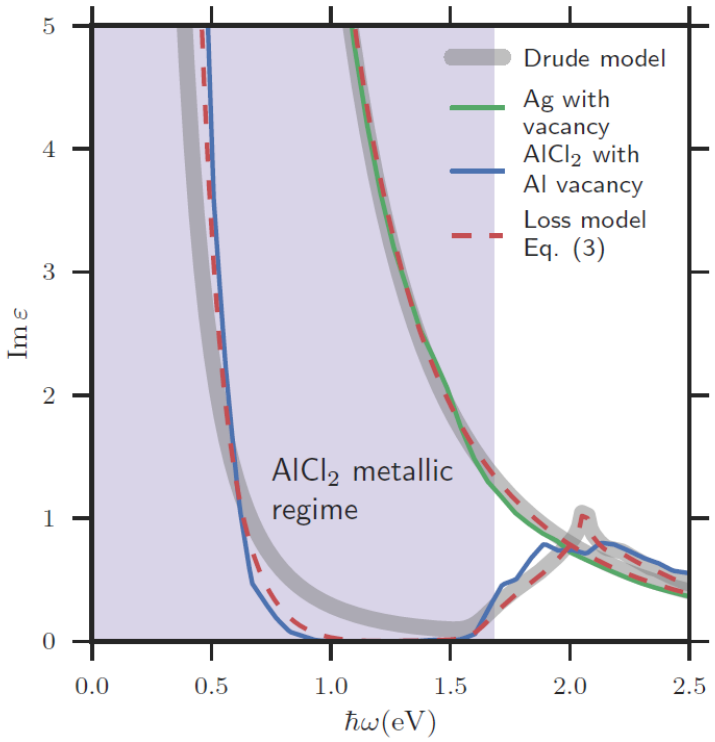

Fig. 10 Defect induced optical losses and energy-dependent relaxation time model. The calculated optical losses (Im ε) for silver (green) and AlCl2 (blue) with a vacancy defect.

As one can see in the range between 1 and 1.5eV the loss in the layered Vand –der-Waals material is much less than Drude model predicts and also much less than in silver. These results confirm our original prediction and in the future we shall continue to work in this direction.

Bibliography

[1] S. A. Maier , *Plasmonics: Fundamentals and Applications* , Springer, Boston, MA **2007** .

[2] J. B. Khurgin, "How to deal with the loss in plasmonics and metamaterials", *Nature Nanotechnology* **10** 2-6, (2015)

[3] A. Boltasseva , H. A. Atwater , "Low-Loss Plasmonic Metamaterials", *Science* **2011** , *331* , 290

[4] A. Boltasseva, "Empowering plasmonics and metamaterials technology with new material platforms", *MRS Bulletin,* 39, **461** (2014)

[5] B. Dastmalchi, P. Tassin, T. Koschny, C. M. Soukoulis, "A New Perspective on Plasmonics: Confinement and Propagation Length of Surface Plasmons for Different Materials and Geometries", *Advanced Optical Materials*, **4** pp 171-184 (2016)

[6] J. D. Caldwell et al, Low-loss, infrared and terahertz nanophotonics using surface phonon polaritons, Nanophotonics, 4, 44-68 (2015)

[7] Jacob B Khurgin "Replacing noble metals with alternative materials in plasmonics and metamaterials: how good an idea?." Phil. Trans. R. Soc. A 375: 20160068 (2017).

[8] M. Stockman, Opt. Express **19**, 22029-22106 (2011)

[9] W. L. Barnes, A. Dereux, and T. W. Ebbesen, Nature **424**, 824 (2003)

[10] N. A. Mortensen, S. Raza, M. Wubs, T. Søndergaard, and S. I. Bozhevolnyi, Nat. Commun. **5** (2014).

[11] U. Kreibig and M. Vollmer, Optical Properties of Metal Clusters (Springer-Verlag, Berlin, 1995).

[12] G. Sun, J. B. Khurgin, and A. Bratkovsky, Phys. Rev, B **84**, 045415 (2011)

[13] G. Sun and J. B. Khurgin, Appl. Phys. Lett. **97**, 263110 (2010)

[14] J. B. Khurgin, G. Sun, "In search of the elusive lossless metal", Appl. Phys. Lett., 96, 181102 (2010)

[15] M. N. Gjerding, K. S. Thygesen, M. Pandey, "Band structure engineered layered metals for low-loss plasmonics", accepted to Nature Commun. (2017)